Short Communication

Propellants, Explosives, Pyrotechnics

DOI: 10.1002/prep.201200142

Preparation and Characterization of Energetic Crystals with Nanoparticle Inclusions

David A. Reese,[a] Steven F. Son,[b] and Lori J. Groven*[b]

Abstract: Energetic crystals with nanoparticle inclusions were preparated and characterized, focusing on the nanosized iron(III) oxide-ammonium perchlorate system, generated using an ethyl acetate/acetone antisolvent:solvent system. It is shown that capture is dependent on antisolvent-to-solvent ratio; increased quantities of antisolvent lead to faster nucleation rates, smaller crystals, and improved capture. Additionally, the crystal habit formation is modified by the addition of nanoparticles, resulting in highly uniform rod-like crystal structures. Results with nanoaluminum-ammonium perchlorate and nanoaluminum-cyclotrimethylenetrinitramine (RDX) systems have shown similar capture behavior.

Keywords: Nanosized Fe_2O_3 · Ammonium perchlorate · RDX · Composite particles

1 Introduction

The addition of nanoparticles to composite propellant formulations theoretically leads to dramatically increased burning rate and combustion efficiency [1,2]. However, nanoparticles have played a severely limited role in modern propellant formulation development thus far because of undesirable resulting properties. The literature is replete with examples of unworkable viscosities during processing, brittle finished products, poor combustion efficiency, and/or combustion stability problems during use [3,4]. These issues ultimately are a result of the high surface area (25–250 $m^2 g^{-1}$) of the nanoparticles preferentially adsorbing the liquid propellant binder components during processing, preventing complete dispersion and reducing the capability of the binder matrix to retain other propellant ingredients.

One proposed means of eliminating these issues while retaining the advantages of nanoparticle inclusion is the capture of the nanoparticles in micrometer-scale energetic crystals. Past efforts have resulted in poorly-characterized crystals, with the bulk of the nanoparticles adhered to the exterior surface of the crystal and overall lack of inclusion [5–7]. This result is driven strongly by the fact that crystallization is a process of purification; impurities within the crystal preferentially remain in solution, as they do not fit within the crystal lattice.

In this work, we investigate the use of a practical, scalable solution crash method to capture Fe_2O_3 nanoparticles within ammonium perchlorate. Fast crash is ideal for such a process, as it drives the solution to the supersaturation limit during crystallization, resulting in an "increasing rate of generation" [8] that enables nanoparticle capture. Characterization of the resulting composite particles is conducted using scanning electron microscopy, particle size analysis, inductively coupled plasma emission spectroscopy, and differential scanning calorimetry/thermogravimetric analysis. The fast crash approach is applicable to several nanoparticle-crystal systems, thus allowing the benefits of particle inclusion to be realized across a multitude of crystalline energetic materials.

2 Experimental Section

2.1 Crystallization

In a typical fast crash process, the following procedure was used. Acetone (100 mL) was chilled in an ice bath at 4 °C. Chemical grade ammonium perchlorate (1.5 g, Sigma-Aldrich, St. Louis, MO) was added and stirred until dissolved. In the acetone/ammonium perchlorate system, reduced temperature results in an increase in the solubility [9]. The nanoscale particles (15 mg of 3 nm NANOCAT® Fe_2O_3, Mach I Chemicals, King of Prussia, PA) were added to this solution. Afterwards, the resulting mixture was bath sonicated (Cole Parmer 8890) for 5 min to disperse the nanoscale Fe_2O_3 (nFe_2O_3) particles. As it warmed, the mixture began to approach, but never surpassed the AP/acetone solubility

[a] *D. A. Reese*
School of Aeronautics and Astronautics
Purdue University
500 Allison Rd, West Lafayette, IN 47907, USA

[b] *S. F. Son, L. J. Groven*
School of Mechanical Engineering
Purdue University
500 Allison Rd, West Lafayette, IN 47907, USA
**e-mail: lgroven@purdue.edu*

limit. After 5 min, the antisolvent (ethyl acetate, 50 mL or 300 mL) was poured directly into the system while rapidly stirring with a spatula to crash the AP crystals onto the $n$$Fe_2O_3$. The solution was placed back into the ice bath for 10 min to force the crystallization to be driven by the antisolvent. Finally, the solution was filtered and dried in a vacuum.

2.2 Analytical Instrumentation

Thermal analysis was conducted with a TA Instruments Q600 simultaneous differential scanning calorimeter/thermogravimetric analyzer (DSC/TGA). A heating rate of $10\,^{\circ}C\,min^{-1}$ was employed under ultra-high purity argon (99.999%) at $100\,mL\,min^{-1}$, with open alumina pans (90 μL). Scanning electron microscopy was conducted with a FEI Nova NanoSEM. A Malvern MasterSizer2000 with a Hydro 2000 μP dispersion unit was used for particle sizing of all materials with hexanes as the carrier solvent. Specific surface area measurements were conducted using the Brunauer, Emmett and Teller method (BET) with a Micromeritics-Tristar 3000. Prior to surface area measurement, the materials were degassed in a nitrogen atmosphere for 2 h at 80 °C. Inductively coupled plasma emission spectroscopy (ICP) was conducted by Galbraith Laboratories, Knoxville, TN. Prior to analysis, samples were sonicated in hexanes using a Branson Model 450 digital sonifier with a Model 102C probe attachment. The material was washed three consecutive times, replacing the dirty solvent with clean (ca. 5 mL) by pipette between washings.

3 Results and Discussion

Scanning electron microscopy images of crystals produced at 0.5 : 1 and 3 : 1 antisolvent-to-solvent ratios, with and without nanoparticle addition, are shown in Figure 1. Higher ratios of antisolvent led to faster crystallization rates, resulting in the formation of crystals with higher aspect ratios. Additionally, nanoscale ammonium perchlorate structures are visible on the surface of the crystals formed without Fe_2O_3 [Figure 1(c)]. The presence of these structures made it difficult to discern the level of inclusion of Fe_2O_3 present in the co-crystallized material by microscopy.

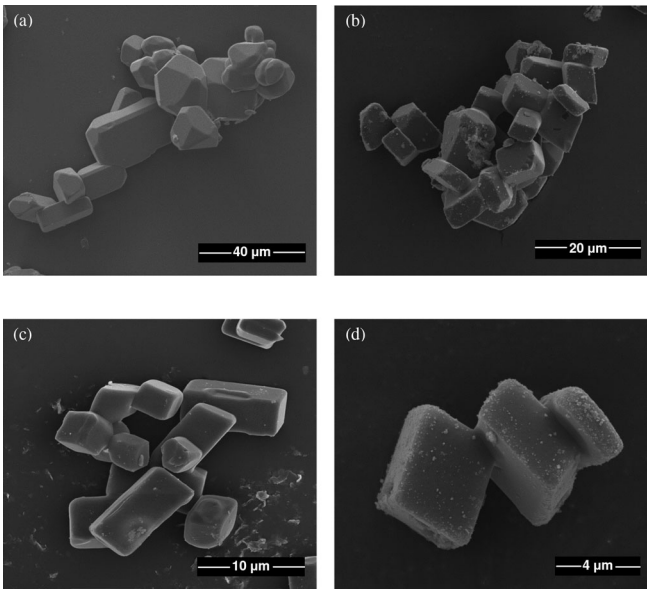

Figure 1. Scanning electron microscopy of (a) 0.5 : 1 (slow crash) AP, (b) 0.5 : 1 AP + 1 wt-% Fe_2O_3 particles – note patches of Fe_2O_3 visible on the surface of the crystals, (c) 3 : 1 (fast crash) AP, (d) 3 : 1 (fast crash) AP + 1 wt-% Fe_2O_3 particles.

Crystals produced using the same process but without nanoparticles formed with both rod-like and prismatic morphologies. When nanoparticles were included in the process, the crystals were nearly uniform in their rod-like morphology. The inclusion of particulate fillers is known to strongly affect the crystal habit [9,10]. The nanoparticles create nucleation sites that encourage even crystal growth throughout the solution. This is in contrast to the crystals formed without nanoparticle inclusion, which nucleated in a somewhat stochastic fashion, resulting in a wider distribution of particle sizes and shapes. Table 1 shows the effect of solvent ratio on mean particle size and specific surface area. Increasing antisolvent ratio decreased the mean size of the crystals produced. This is consistent with behavior shown in previous work [11]. However, when comparing the specific surface areas of the composite particles, the larger crystals produced by the low nucleation rate process had a higher surface area than the smaller crystals produced by the high nucleation rate process. This increase in surface area is caused by reduced capture of the nanoparticles. At low nucleation rates (e.g., those

Table 1. Volume-weighted mean particle sizes and specific surface areas for low-rate (0.5 : 1) and high-rate (3 : 1) AP, AP + 1 wt-% Fe_2O_3 composite particles, and physically mixed AP + 1 wt-% Fe_2O_3.

	0.5 : 1 AP (neat)	0.5 : 1 AP + Fe_2O_3 (comp)	0.5 : 1 AP + Fe_2O_3 (mixed)	3 : 1 AP (neat)	3 : 1 AP + Fe_2O_3 (comp)	3 : 1 AP + Fe_2O_3 (mixed)
$D_{4,3}$/μm	148	71	86	56	25	14
SSA/$m^2\,g^{-1}$	1.253	4.016	6.129	1.087	2.596	11.250
Fe content/%	–	0.391	–	–	0.646	–

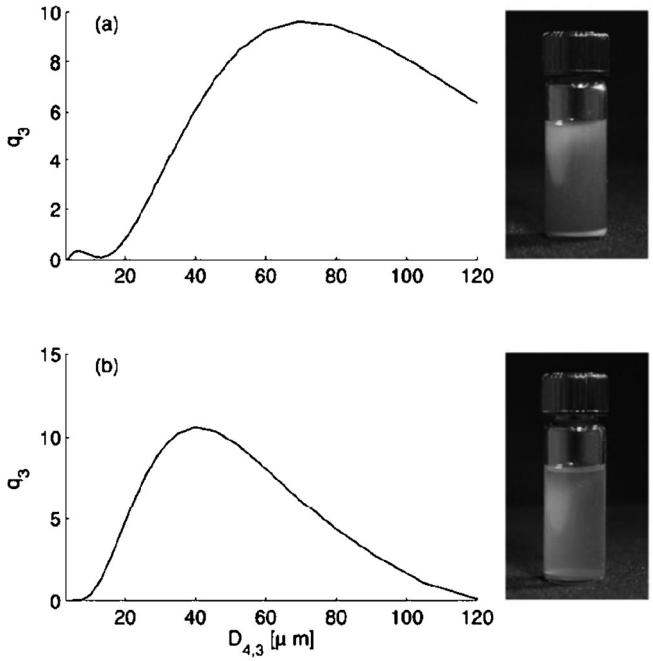

Figure 2. Volumetric size distribution q_3 and results of sonic washing of (a) 0.5 : 1 (slow crash) AP + 1 wt-% Fe_2O_3 and (b) 3 : 1 (fast crash) AP + 1 wt-% Fe_2O_3 composite particles, in 1 dram vials. Suspended nanoparticles are visible in both the laser diffraction size distribution and the liquid above the particles in the 0.5 : 1 system.

driven by 0.5 : 1 antisolvent-to-solvent ratios), the nanoparticles are rejected from the crystal structure and lay agglomerated on the surface of the crystals [Figure 1(b)]. This type of surface agglomeration has also been noted by researchers in a HMX–carbon nanotube system produced by crash precipitation [9].

To further assess the level of nanoparticle capture, samples of low and high nucleation rate composite crystals were bath sonicated in hexane. As shown in Figure 2, the particles on the surface of the low nucleation rate crystals were dispersed into the hexane – a result distinctly different from that generated by the solution containing high nucleation rate crystals, in which little apparent dispersion was noted. Note that the 0.5 : 1 system vial contains extremely cloudy solution atop bright white crystals, while the 3 : 1 system vial contains relatively clear solution atop coral colored crystals.

When the low nucleation rate particles are examined using laser diffraction – also in hexane – the detached nanoparticles appear in the sub-micrometer region of the size distribution measurement. This sub-micrometer peak does not appear in the analysis of the high nucleation rate particles. Size distributions and images of sonicated vials for low and high rate composite particles are also shown in Figure 2. Quantitative assessment of the level of capture was determined with ICP. Baseline measurements were accomplished by assessing crystals with 1 wt-% Fe_2O_3 added by simple physical mixing. The resulting iron content measured was 0.646 % (or 0.935 wt-% Fe_2O_3). At low nucleation rates (0.5 : 1 antisolvent-to-solvent) the level of capture was only around 60 % (0.391 % Fe), while for high nucleation rates (3 : 1 antisolvent-to-solvent) the level of capture was over 92 % (0.601 % Fe). These results are also summarized in Table 1. Some preliminary results with nanoaluminum–ammonium perchlorate and nanoaluminum–RDX show that other particle-crystal systems are amenable to this process as well.

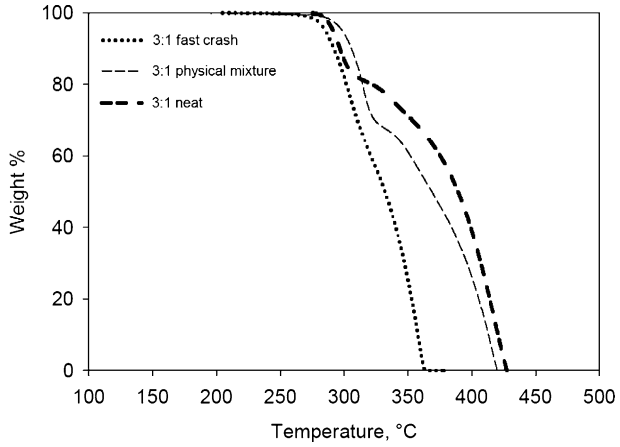

Figure 3. TGA analysis of 3 : 1 AP + Fe_2O_3 composite particles, 3 : 1 AP + Fe_2O_3 physical mixture, and 3 : 1 AP alone. The composite particles decomposed at the lowest temperature, as they exhibited the most intimate contact between the Fe_2O_3 catalyst and the AP.

Thermal decomposition behavior for the fast nucleation rate crystals is presented in Figure 3. The fast nucleation case clearly illustrates that the inclusion of $n$$Fe_2O_3$ drastically alters the decomposition behavior of the AP crystals; for this material, decomposition is complete at ca. 360 °C, nearly 55 °C below that of either neat crystals or physical mixtures of $n$$Fe_2O_3$ and AP. This falls within the expected range of decomposition temperatures for Fe_2O_3-catalyzed AP particles previously reported in the literature [12]. Though not shown, for a 0.5 : 1 antisolvent-to-solvent ratio, we did not observe any shift in decomposition temperature with $n$$Fe_2O_3$ addition.

4 Conclusions

Iron(III) oxide nanoparticles were successfully included in crystals of ammonium perchlorate using a fast solution crash method. The resulting composite crystals were characterized using scanning electron microscopy, laser diffraction, surface area analysis, DSC/TGA, and inductively coupled plasma emission spectroscopy. Inclusion was most successful at the high crystallization rates generated by high antisolvent-to-solvent ratios.

By including the nanoparticles within the crystals, a significant decrease was noted in the specific surface area of the composite particles vis-à-vis a physical mixture of the con-

stituent ingredients. Quantitative analysis indicates that, at high crystallization rates, a capture level of 92% is possible. This result should help enable the inclusion of nanoparticles in propellant formulations, while minimizing the surface area-related drawbacks. Our preliminary results with nanoaluminum–ammonium perchlorate and nanoaluminum–RDX indicate that other particle-crystal systems are amenable to this process as well. The inclusion of nanoparticles within energetic materials provides potential to create explosives or propellants with possibly reduced sensitivity and highly tunable ignition and combustion mechanisms.

Acknowledgments

The authors would like to acknowledge funding from *Dr. Mitat Birkan* of the Air Force Office of Scientific Research, under contract numbers FA9550-11-1-0002 and FA9550-09-C-0176. Also, the authors would like to thank *Debby Sherman* of the Purdue Life Science Microscopy Facility for providing imaging.

References

[1] A. Dokhan, E. W. Price, R. K. Sigman, J. M. Seitzman, The Effects of Al Particle Size on the Burning Rate and Residual Oxide in Aluminized Propellants, *37th AIAA/ASME/SAE/ASEE Joint Propulsion Conference*, Salt Lake City, UT, USA, July 8–11, **2001**, AIAA 2001–3581.

[2] L. Galfetti, L. T. DeLuca, F. Severini, L. Meda, G. Marra, M. Marchetti, M. Regi, S. Bellucci, Nanoparticles for Solid Rocket Propulsion, *J. Phys. Condens. Mater.* **2006**, *18*, S1991 – S2005.

[3] R. A. Yetter, G. A. Risha, S. F. Son, Metal Particle Combustion and Nanotechnology, *Proc. Combust. Inst.* **2009**, *32*, 1819 – 1838.

[4] J. Zhi, L. Shu-Fen, Z. Feng-Qui, L. Zi-Ru, Y. Cui-Mei, L. Yang, L. Shang-Wen, Research on the Combustion Properties of Propellants with Low Content of Nano Metal Powders, *Propellants Explos. Pyrotech.* **2006**, *31*, 139 – 147.

[5] Z. Ma, F. Li, H. Bai, Effect of Fe_2O_3 in Fe_2O_3/AP Composite Particles on Thermal Decomposition of AP and on Burning Rate of the Composite Propellant, *Propellants Explos. Pyrotech.* **2006**, *31*, 447–451.

[6] X. Holmbäck, Ă. C. Rasmuson, Size and Morphology of Benzoic Acid Crystals Produced by Drowning-Out Crystallization, *J. Cryst. Growth* **1999**, *198*, 780 – 788.

[7] A. E. D. M. Vanderheijden, R. H. B. Bouma, A. C. van der Steen, H. R. Fischer, Application and Characterization of Nanomaterials in Energetic Compositions, *Mater. Res. Soc. Symp. Proc.* **2004**, *800*, 191 – 210.

[8] Z. Ma, C. Li, R. Wu, R. Chen, Z. Gu, Preparation and Characterization of Superfine Ammonium Perchlorate (AP) Crystals through Ceramic Membrane Anti-Solvent Crystallization, *J. Cryst. Growth* **2009**, *311*, 4575 – 4580.

[9] P. M. McGenity, J. J. Hooper, C. D. Paynter, A. M. Riley, C. Nutbeem, N. J. Elton, J. M. Adams, Nucleation and Crystallization of Polypropylene by Mineral Fillers: Relationship to Impact Strength, *Polymer* **1992**, *33*, 5215–5224.

[10] Q. Yuan, V. G. Rajan, R. D. K. Misra, Nanoparticle Effects During Pressure-Induced Crystallization of Polypropylene, *Mater. Sci. Eng. B* **2008**, *153*, 88 – 95.

[11] B. B. Glover, W. Lee Perry, Observation of Localized Charge Transport in Isolated Microscopic Mats of Single-Wall Carbon Nanotubes, *J. Appl. Phys.* **2007**, *101*, 064309.

[12] V. V. Boldyrev, Thermal Decomposition of Ammonium Perchlorate, *Thermochim. Acta* **2006**, *443*, 1 – 36.

Received: August 30, 2012
Revised: September 14, 2012

